The significance of two-phase plasticity for the crack initiation process during very high cycle fatigue of duplex steel

Alexander Giertler[1,*], Marcus Söker[1], Benjamin Dönges[2], Konstantin Istomin[2], Ullrich Pietsch[2], Claus Peter Fritzen[2], Wolfgang Ludwig[3], Hans-Jürgen Christ[2], Ulrich Krupp[1]

[1] Faculty of Engineering and Computer Science, University of Applied Sciences Osnabrück, 49009 Osnabrück, Germany
[2] Faculty IV: Science and Technology, University of Siegen, 57068 Siegen, Germany
[3] European Synchrotron Radiation Facility, 38000 Grenoble, France
* Corresponding author: a.giertler@hs-osnabrueck.de

Abstract   The present paper reviews experimental results on the fatigue damage of grade 1.4462 austenitic-ferritic duplex steel in the very high cycle fatigue (VHCF) regime. Electrolytically polished miniature and bulk specimens have been fatigued in an ultrasonic fatigue testing machine while the surface is observed in-situ by an optical microscope. The pre-fatigued miniature specimens are investigated by synchrotron diffraction contrast tomography (DCT) to reveal three-dimensional crystallographic orientation data. These data are used for finite element modeling in combination with a material model accounting for elastic anisotropy and crystal plasticity to predict crack initiation sites. The bulk specimens are carefully analyzed by means of scanning electron microscopy (SEM) in combination with electron back-scatter diffraction (EBSD). Under VHCF loading conditions, slip band formation is limited to the softer austenite grains – in particular at twin boundaries. Once being formed, the bands generate high stress concentrations where they impinge the austenite-ferrite ($\gamma-\alpha$) phase boundaries, eventually, leading to crack initiation. The results are discussed by means of a numerical modeling approach that is based on (i) the finite element method (FEM) mentioned above and (ii) a crack initiation model proposed by Tanaka and Mura [1] and Chan [2].

Keywords   Duplex steel, VHCF, short fatigue cracks

1. Introduction

The fatigue life of metallic materials is determined by the plastic strain amplitude. The amplitude level determines the effective damage mechanism. For example, during LCF loading an early formation of slip bands can be observed, which leads to initiation and formation of long fatigue cracks [3]. In the HCF regime, the macroscopic strain amplitude is lower, but the microscopic strain amplitude can reach a critical value due to the elastic anisotropy of the microstructure, which results in the formation and propagation of microstructurally short fatigue cracks. In the VHCF range, the initiation and propagation of fatigue cracks is mainly influenced by the microstructure. Therefore, a large scatter can be observed in the fatigue life data. Life-determining factors are size, shape and distribution of non-metallic inclusions and the ability of grain and phase boundaries to block cyclic slip or microcracks. Duplex stainless steels exhibit a good combination of high strength, ductility and corrosion resistance [4]. Many applications imply cyclic loading, for instance the power transmission in off-shore boats. To ensure the reliability of such machines the knowledge about the fatigue behavior is essential. The assessment of the fatigue life is usually based on Wöhler data, but environmental effects, single overloads or the influences of varying microstructural impurities are often not taken into account, which leads to a non-conservative prediction. The present paper gives some evidences about the fatigue damage mechanism for ferritic austenitic duplex stainless steel in the VHCF regime and supports the hypothesis that phase boundaries act as effective barriers against fatigue crack initiation.

2. Experimental Procedure

The behavior of microstructurally short fatigue cracks were investigated in the VHCF regime on the austenitic ferritic duplex stainless steel DIN 1.4462. Duplex steel exhibit good strength and ductility values paired with excellent corrosion resistance [4]. The chemical composition of the material and the heat treatment pa-

rameters for the homogenizing and grain coarsening (required for 3D synchrotron tomography) is given in Table 1.

Table 1: Chemical composition of the duplex steel (wt. %) and heat treatment parameters.

C	Cr	Ni	Mo	Mn	N	P	S	Fe
0.02	21.9	5.6	3.1	1.8	0.19	0.023	0.002	bal.

grain coarsening	1250°C (4h); cooling down to 1050°C (1K/min); water quench
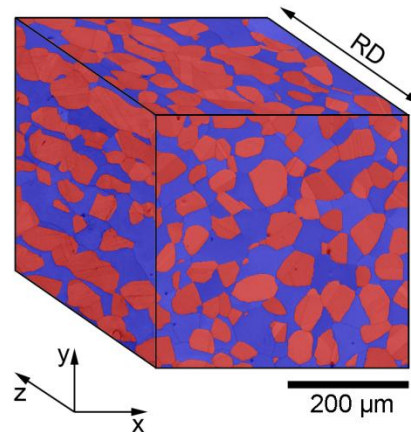
Figure 1: Microstructure of the investigated stainless duplex steel, austenite (red), ferrite (blue).

The grain coarsening heat treatment resulted in a microstructure consisting of 50 % austenite and 50 % ferrite, with a mean grain size of 33 µm for austenite and a mean grain size of 41 µm for ferrite. The geometries of the specimens are given in Figure 2; (a) shows the cylindrical bulk specimen, (b) shows the miniature specimen which has been developed for the synchrotron experiments at ESRF Grenoble. Both kinds of specimens are electro-polished in the gauge length; therefore, the surface of the specimens can be observed by means of light and electron microscopy in combination with automated electron back-scatter diffraction (EBSD).
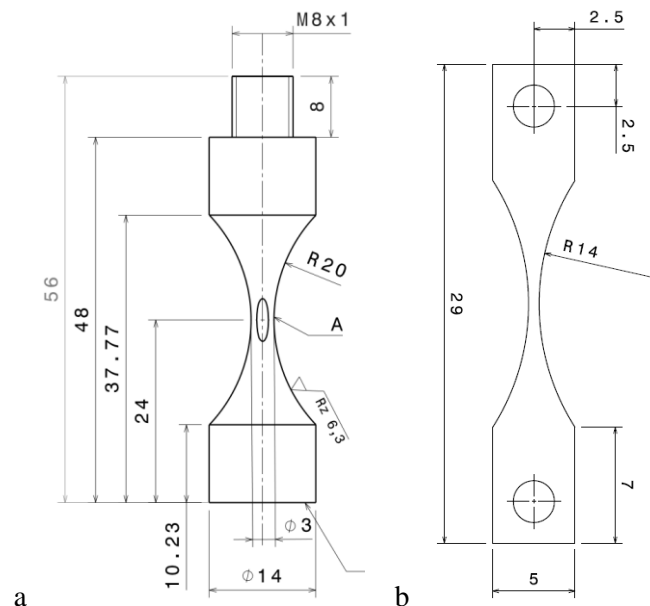
Figure 2: (a) shallow notched specimen for the VHCF tests, (b) flat bone shaped specimen for the VHCF tests.

For the cyclic loading of the samples an ultrasonic fatigue testing equipment designed and produced by BOKU Vienna was used, with an average frequency of f = 20 kHz and an load ratio of R = -1. To prevent heating of the specimens during cycling compressed air cooling is used. The observation of the fatigue dam-

age within the machine is done with an optical far field microscope Questar QM100. The microscope is focused on the shallow notched area in the middle of the gauge length of the specimen shown in Fig. 2 (a). The microscope is continuously taking pictures of the surface, thus a measurement of the crack growth is possible. The miniature specimens are used for phase contrast tomography (PCT) and the relatively new developed diffraction contrast tomography (DCT) to map the grain microstructure in the gauge length of the specimen. The digital reconstruction of the three-dimensional volume contains the grain shape and distribution and also the crystallographic orientation data of every individual grain. By using these data, it is possible to calculate the stress distribution within the two-phase microstructure by means of the finite element method (FEM) in combination with an elastic-anisotropic, crystal-plastic material model.

3. Results

The fatigue tests were carried out under uniaxial tension-compression (R=-1) at room temperature. As it was found in certain studies [5], a strong slip band formation in the austenite grains took place during the tests. The sample shown in Figure 3 was loaded with an stress amplitude of $\Delta\sigma/2$=400 MPa up to $1.6 \cdot 10^6$ cycles until the test was stopped. The crack initiation took place at a $\gamma-\alpha$ phase boundary between the grains 1 and 3. The crack initiation site has been analyzed by EBSD to calculate the corresponding slip systems and Schmid factors. For the austenite grain 1 a Schmid factor of M_s=0.46 was determined and the slip planes in grain 1 are oriented in the $(11\bar{1})$ direction; in comparison, the ferrite grain 3 has an corresponding Schmid factor of M_s=0.35. During the test, grain 1 shows a continuously increasing number of activated slip bands, thus it seems that the cracking of the phase boundary in this case is depending on the amount of accumulated micro strain caused by the local plastic deformation of grain 1.
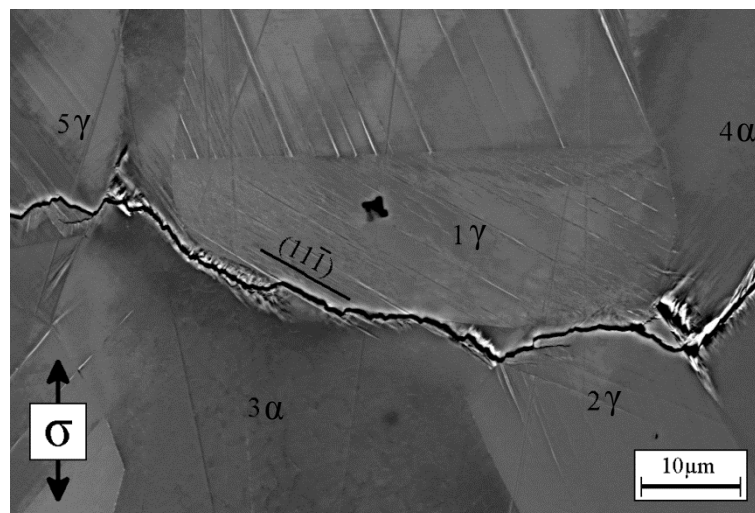
Figure 3: Crack initiation site of a fatigue sample loaded at $\Delta\sigma/2$=400MPa, $1.6 \cdot 10^6$ cycles.

Figure 4 shows the optically measured crack length vs. the number of cycles for the left and right crack front. The crack shown in Figure 3 corresponds only to the first 50 μm of the final crack length. The crack length is measured starting from its crack initiation site to the left and right direction, to show the varying crack propagation rates being visible at the surface. It was found that the propagating crack follows within the first $1.3 \cdot 10^6$ cycles the phase boundary in the left direction until it reaches grain 5. In the other direction it took the same number of cycles to overcome the grain boundary between grain 1 and grain 2 to reach grain number 4. The crack propagation starts to accelerate after the crack crosses the phase boundaries to the grains 4 and 5. The individual crack propagation rate was calculated for grains 4 and 5. For the ferrite grain 4 the rate was $1.1 \cdot 10^{-9}$ m/cycle, the rate for the austenite grain 5 was lower with $4.5 \cdot 10^{-10}$ m/cycle. This effect can be correlated to the different kinds of active slip mechanisms in austenite and ferrite. One possible explanation of this discrepancy between the different crack propagation rates in austenite and ferrite could be the splitting of the energy on multiple slip systems (= lower da/dN in austenite), which is necessary for local plastic deformation [5].
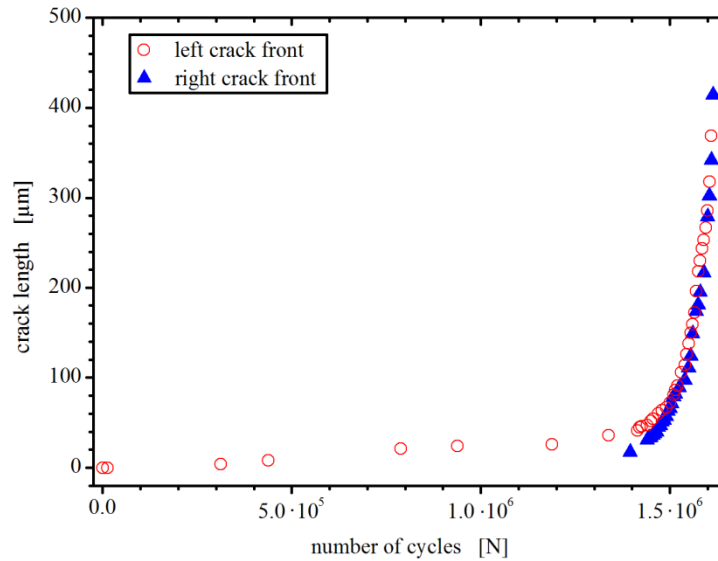
Figure 4: Crack length vs. the number of cycles for the left and right crack front.

The crack shown in Figure 5 initiated at the phase boundary between the austenite grain 3 and the ferrite grain 1. The specimen was loaded with a stress amplitude of $\Delta\sigma/2=400$ MPa up to $1.7\cdot10^6$ cycles until the test was stopped manually to prevent the breaking of the specimen.
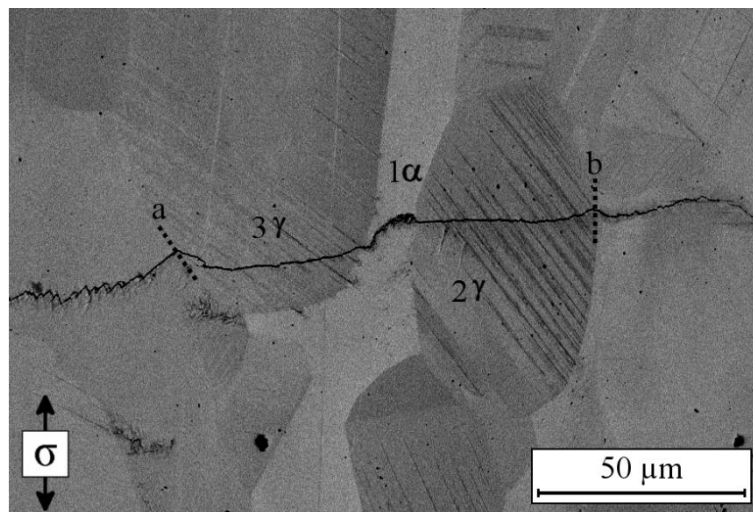
Figure 5: Crack path of a fatigue sample loaded at $\Delta\sigma/2=400$MPa, $1.7\cdot10^6$ cycles.

By analyzing the micrographs which have been taken every thousand cycles during the fatigue test, it was possible to reconstruct the crack propagation path. In this case, the crack spends about $1.3\cdot10^6$ cycles to cross the ferrite grain 1, starting from its initiation site and propagating in the direction of austenite grain 2 at an angle of about 45°with respect to the stress axis. This first part of the crack propagation process is quantified in Figure 6. After reaching the austenite grains 2 and 3, the crack is changing its propagation direction perpendicular to the stress axis by changing its slip mechanism into double slip.
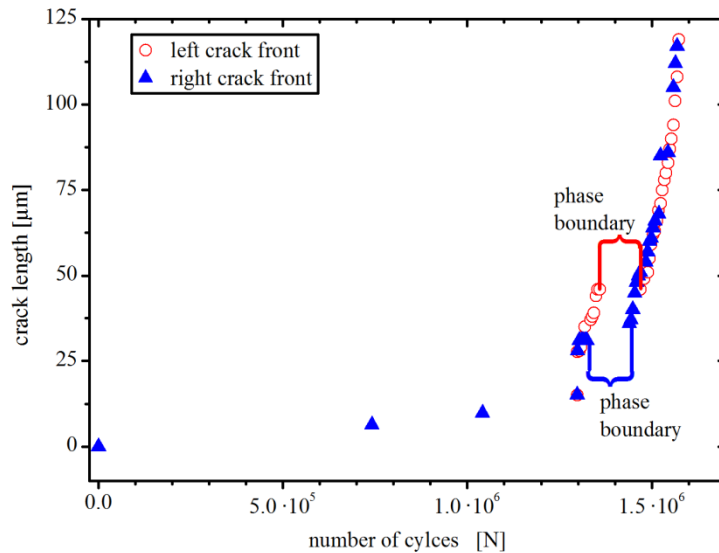
Figure 6: Crack length vs. the number of cycles for the left and right crack front

After crossing the austenite grains 2 and 3, the crack reaches the phase boundary marked with an "a" and "b" in Figure 5. Obviously, the phase boundary acts as an effective barrier against crack propagation, what is supported by the crack length data in Figure 6. This effect is caused by the incompatibility of the slip systems between neighboring grains [6]. The data from the crack length measurement was further analyzed to calculate the fatigue crack propagation rate of the left crack front as a function of the crack length, cf. Figure 7. The plotted data reveals that when approaching the phase boundary the crack propagation rate decreases down to da/dN≈0 and the crack arrests at the phase boundary. After crossing the phase boundary, the crack propagation rate increases again.
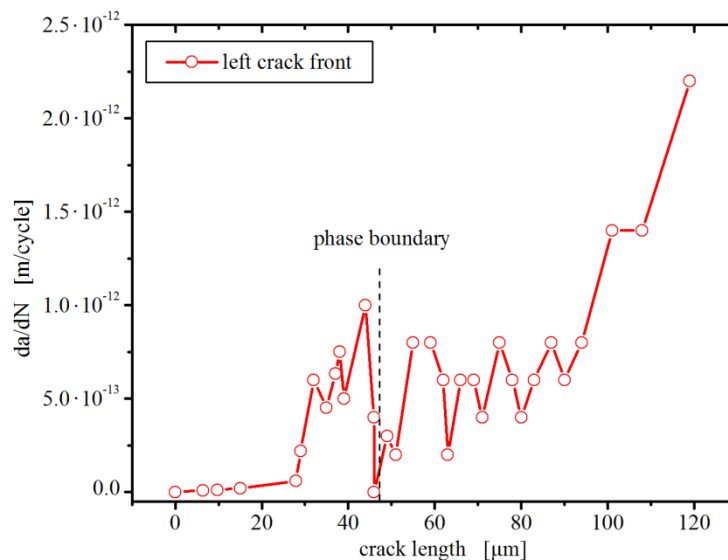
Figure 7: Crack propagation rate vs. the crack length for the left crack front in Fig. 5.

However, the observation by means of light microscopy can only reveal information about crack initiation and propagation processes that can be related to the surface grains of a specimen. In case of VHCF loading, the three-dimensional microstructure needs to be taken into account. Therefore, miniature specimens that can be attached to a titanium carrier for fatigue testing in an ultrasonic fatigue testing machine were developed to get three-dimensional information about the duplex microstructure by means of synchrotron tomography under cyclic loading. The experiments are done using the phase-contrast tomography (PCT) and the diffraction-contrast tomography (DCT). DCT is a new developed method which gives the possibility to image the 3D grain structure with its crystallographic orientation data, Figure 8 a. The specimen is placed in the beam

very close to the detector plane.
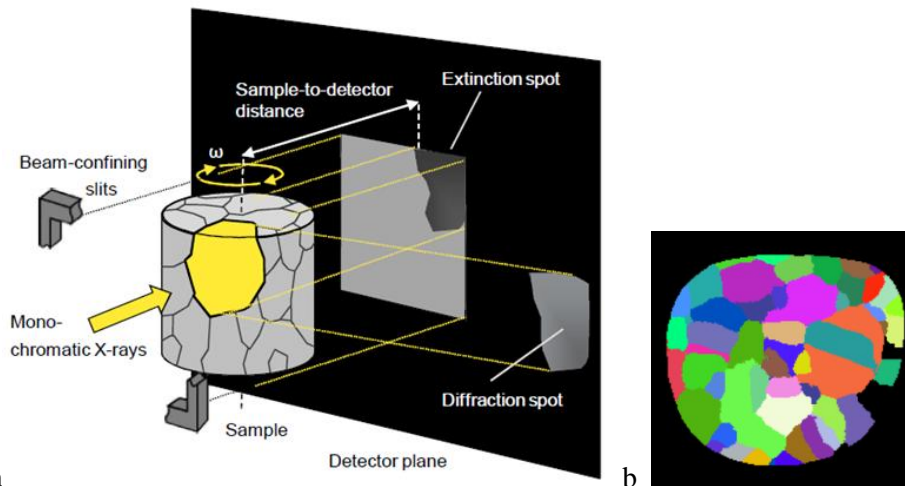
Figure 8: (a) Illustration of the working principle of the diffraction-contrast tomography (DCT) [7], (b) reconstructed slice of a duplex steel fatigue specimen mapped with DCT.

The beam is confined by slits to limit the number of penetrated grains. During the rotation of the sample, some of the grains fulfill the Bragg condition; therefore, the grains are producing diffraction spots on the detector plane. Afterwards, a semi-automated computer code reconstructs the individual grain shape and position in the volume from the pictures taken during the rotation of the sample, cf. Figure 8 b.

The data will be used for a more detailed prediction of local crack or slip band nucleation sites by means of the finite-element method (FEM). An example of the application of the FEM is given in Figure 9. The microcracks (see arrows in Figure 9 a) were initiated at a stress amplitude of $\Delta\sigma/2=365$ MPa. The emanation process of the slip bands within the austenite grain γ_1 leads to stress intensities at the phase boundaries and in the neighboring ferrite grain α_1.
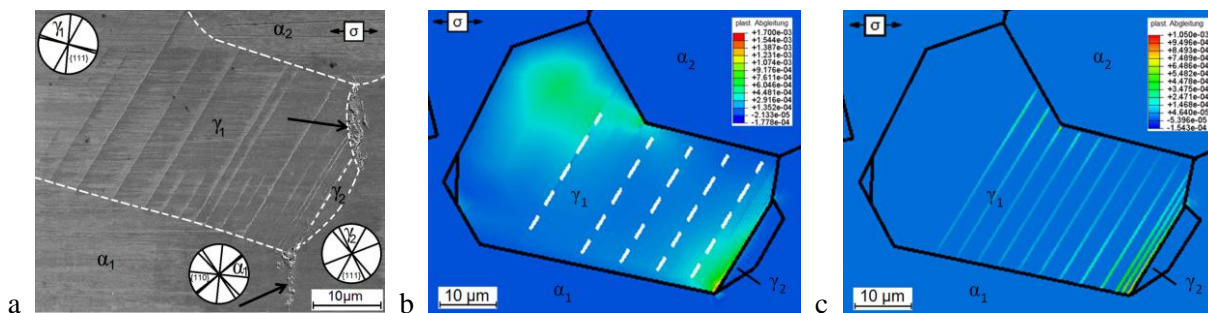
Figure 9: (a) intercrystalline und transcrystalline fatigue crack initiation (arrows) in the ferrite, introduced by local stress intensities caused by slip bands within the austenite, (b) plastic slip on the slip system with the highest stress, (c) plastic slip on discrete slip bands.

Eventually, the initiated dislocation motion in the ferrite leads to the crack initiation process described by Tanaka and Mura [1]. The transport of the plastic deformation was supported by the low twist and tilt angle between the austenite γ_1 and ferrite α_1 grains. With the help of a material model according for crystal plasticity, the slip on adjacent slip systems have been calculated by FEM [8]. The model is considering the elastic and plastic anisotropic deformation of the grains, which is leading to the inhomogeneous stress distribution. Figure 9 b shows the displacement on slip system in the austenite grain γ_1 with the highest stress, leading to pronounced slip band formation. To analyze the stress distribution at the phase boundaries, discrete slip bands have been integrated on the highly stressed austenite grain (cf. Figure 9 c), according to the results of Figure 9 b. These slip bands are activated when the local friction stress τ_{fr} is exceeded. Meanwhile, the other areas of the austenite grain are deforming only anisotropic-elastic. This approach allows to calculate a global stress value which is not sufficient to initiate any plastic deformation within the ferrite phase. Accordingly, the endurance limit for a certain area of the microstructure can be estimated.

4. Discussion

According to the results of the ultrasonic fatigue tests, it is shown that right at the beginning of fatigue loading local plastic deformation is concentrated in the austenite phase, caused by the elastic anisotropy of the duplex microstructure. Slip band formation within the austenite grains, produces strong dislocation pile ups at the phase boundaries. These local stress intensities are predominant sites for crack initiation (cf. Figure 3). The crack propagation process was observed by means of a far field microscope to correlate the crack path with its surrounding microstructure. The α/γ-phase boundary has been identified as an effective barrier against fatigue crack propagation, cf. Figure 7. By knowing the local phase and crystal orientation distribution, e.g., from EBSD measurements, it is possible to predict crack initiation sites in the microstructure by means of FEM. Here, a material model is required that accounts for elastic anisotropy and crystal plasticity. The calculated local shear stresses correlate with initiation sites for slip bands and cracks. As a subject of ongoing work, the 3D data from the diffraction-contrast-tomography experiments will be used for a more precise FEM prediction of slip band and crack initiation sites in the mapped volume. As described earlier, plastic deformation located in the slip band has been found also in the austenite grains even after 10^8 cycles due to the elastic anisotropy of the material. To model the fatigue crack initiation in the VHCF regime the focus has been placed on the evolution of slip bands, and in particular especially on the slip transmission in the neighboring grains and the crack initiation. The underlying model concept follows the work of Tanaka and Mura [1] on crack initiation along slip bands. It describes the fatigue-crack initiation by the accumulation of dislocation dipoles during strain cycling

$$N_i \approx \frac{4Gw_s}{\pi(1-\nu)} \frac{1}{d(\Delta\tau - 2\tau_{fr})^2},$$ (1)

where N_i is the number of cycles for crack initiation, G the shear modulus, w_s the specific fracture energy per unit area along the slip band, ν the Poisson ratio, d the grain size, $\Delta\tau$ the shear-stress range and τ_{fr} the friction stress of dislocation motion. The model was modified for instances by Chan [2], who added the slip band height h and a factor for the cyclic slip irreversibility λ. For the HCF and VHCF regime, where low stress amplitudes are applied, cyclic slip consist of a reversible and irreversible fraction of dislocation movement. The number of cycles N_i for initiation of a crack of length c can be calculated as follows:

$$N_i \approx \frac{8G^2}{\lambda\pi(1-\nu)} \left(\frac{h}{d}\right)^2 \left(\frac{c}{d}\right) \frac{1}{(\Delta\tau - 2\tau_{fr})^2}.$$ (2)

Furthermore, it was shown that slip transmission from one grain to the neighboring grain plays an important role in crack initiation and propagation. This barrier and its effectiveness can be described by the twist and tilt angles of the adjacent slip planes [6, 9].

5. Conclusion

Under fatigue loading, plastic deformation is concentrated in the austenite phase by the emanation of intense slip bands. The formation of slip bands was observed already during the first thousand cycles, leading to local stress intensities at the phase austenite-ferrite boundaries. These areas have been identified experimentally by light microscopy and numerically by the finite element method as critical crack initiation sites. On the other hand, the results are showing that crack initiation is depending to a great extent on the configuration of the tilt and twist angles of the neighboring grains. They control the transport of the local plastic deformation concentrated on the slip bands in the austenite across the phase boundary into the ferrite phase. This effect supports the assumption that VHCF damage depends on the microstructure. Therefore, understanding of the fatigue mechanisms in the VHCF regime requires the knowledge about the microstructure. Anyhow, in case of crack initiation the cracking of the first grain is dominating the lifetime of the specimens. Furthermore, the experimental data from the fatigue experiments shows that phase boundaries play a major role in fatigue crack propagation. They exhibit the ability to slow down or to stop the crack propagation process. This effect is depending on the configuration of the tilt and twist angles of the slip systems of neighboring grains. A close look on the results show that crack initiation and propagation is a three-dimensional problem.

Hence, a set of miniature fatigue specimens have been fatigued with an ultrasonic fatigue testing machine and afterwards analyzed by means of synchrotron tomography. It is planed that these test data should assist in the near future the FE modeling.

Acknowledgements

References

[1]   K. Tanaka, T. Mura: A Dislocation Model for Fatigue Crack Initiation, J. Applied Mech., 48 (1981) 63.

[2]   K.S. Chan: A Microstructure-Based Fatigue Crack Initiation Model, Met. Mat. Trans. A, 34A (2003) 43.

[3]   M. C. Marinelli: Activated slip systems and microcrack path in LCF of a duplex stainless steel, Mat. Sci. Eng. A, 509, (2009), 81.

[4]   B.I. Voronenko: Austenitic – Ferritic Stainless Steels: A State-Of-The-Art Review, Met. Sci. and Heat Treatm. 39 (1997) 428.

[5]   O. Düber, Untersuchung zum Ausbreitungsverhalten mikrostrukturell kurzer Ermüdungsrisse in zweiphasigen metallischen Werkstoffen am Beispiel eines austenitisch-ferritischen Duplexstahls, PhD Thesis, University of Siegen 2007.

[6]   T. Zhai: The grain boundary geometry for optimum resistance to growth of short fatigue cracks in high strength Al-alloys, Int. J. Fatigue, 27 (2005) 1202.

[7]   M. Herbig: 3-D growth of a short fatigue crack within a polycrystalline microstructure studied using combined diffraction and phase-contrast X-ray tomography, Acta Mater. 59 (2011) 590.

[8]   Y. Huang: A User-Material Subroutine Incorporating Single Crystal Plasticity in the ABAQUS Finite Element Program, Mech Report 178, Division of Engineering and Applied Sciences, Harvard University, Cambridge, 1991.

[9]   W. Schaef: A 3-D view on the mechanisms of short fatigue cracks interacting with grain boundaries, Acta Mater., 59 (2011) 1849.